International Journal of Computational and Experimental Science and Engineering (IJCESEN)

Vol. 11-No.4 (2025) pp. 4814-4821
http://www.ijcesen.com

ISSN: 2149-9144

Copyright © IJCESEN

Research Article

Performance evaluation of U-pipe type evacuated tube collector at low air flow rates: An experimental study

Satish Kumar Gavel[1*], Gajendra Kumar Agrawal[2], T.V. Arjunan[3], Indulata Kanwar[4]

[1]Department of Mechanical Engineering, Government Engineering College Bilaspur (CG,) India
* **Corresponding Author Email:** gavel.satish@gmail.com-**ORCID:** 0000-0002-4953-2222

[2]Department of Mechanical Engineering, Government Engineering College Bilaspur (CG,) India
Email: gajendr2a@gmail.com-**ORCID:** 0000-0002-4953-2222

[3] Department of Mechanical Engineering, GGV Koni (a central university), Bilaspur (CG,) India
Email: arjuna2n@gmail.com-**ORCID:** 0000-0002-4953-2222

[4] Department of Mechanical Engineering, GGV Koni (a central university), Bilaspur (CG,) India
Email: indulat2a@gmail.com-**ORCID:** 0000-0002-4953-2222

Article Info:

DOI: 10.22399/ijcesen.5472
Received: 14 July 2025
Revised: 26 August 2025
Accepted: 10 September 2025

Keywords

ETC
Temperature rise,
Thermal efficiency
Copper fin temperature
Pressure drop

Abstract:

Solar energy is regarded as one of the most favoured forms of renewable energy. Different researchers have proposed various kinds of solar collectors with distinct design changes and operating conditions. Among different types of solar collectors, the evacuated tube collector (ETC) stands out due to its significantly low convective heat losses from the absorber plate. The U-pipe setup within the evacuated tube is popular because of its straightforward design and ability to withstand the high pressure of the working fluid. Numerous theoretical and experimental investigations of U-pipe type ETC with diverse design alterations have been conducted by different researchers. An effort is made to assess the efficiency of a U-pipe type ETC for air flow rates between 1 kg/hr to 4 kg/hr. Experiments were conducted in Bilaspur, Chhattisgarh, India, during four distinct months from November 2024 to May 2025. The monthly average values of peak solar intensities were recorded as 950 W/m^2, 973 W/m^2, 1055 W/m^2, and 1088 W/m^2 for the months of November, February, April, and May, respectively. The peak rise in air temperature and the highest temperatures of copper fins were recorded at 63.7 °C and 179.9 °C, respectively, which corresponded to a mass flow rate of 1 kg/hr for the month of May; however, the greatest thermal efficiency observed was 36.6% at 4 kg/hr in the April. The maximum values of pressure drop and blower power were determined to be 0.30 KPa and 0.31 W, respectively, at a mass flow rate of 4 kg/hr.

1. Introduction

Over the past several decades, the problems of reducing fossil fuels and the emissions produced by them have prompted researchers worldwide to intensify their focus on renewable energy sources. Oil and natural gas will be exhausted first, ultimately followed by coal [1]. Numerous alternative energy sources can replace fossil fuels. The choice of which energy source to use in each instance must be determined by economic, environmental, and safety factors. Due to its favourable environmental and safety features, many believe solar energy should be harnessed over other alternative energy sources, as it can be provided sustainably without damaging the environment [2]. Numerous researchers have explored ETC through both experimental and computational methods with various alterations. Bakry et al. [3] investigated the performance of ETC both with and without SPC for air heating purposes through experimentation. They employed two identical ETC as separate collector units with an outer glass tube diameter of 58 mm and a length of 1.8 m. A copper tube with a diameter of 16 mm was positioned concentrically within the ETC up to a length of 1.6 m. In the ETC units, cold air is directed into the tube and permitted to exit through the annular space between the copper and inner glass tubes. They achieved maximum temperature increases of 100°C and 60°C at low flow rates with

and without the use of CPC, respectively. Wang et al. [4] introduced a combined collector-storage SAH system. They employed an evacuated tube for collection and utilized paraffin as the storage medium and heat transfer fluid (HTF). They suggested a conceptual structure with a roof area of 9.9 m2 using this system along with an additional electric heater. They achieved a yearly energy saving of 4039.3 MJ and a reduction in carbon emissions of 5792.8 kg. Singh et al. [5] employed an evacuated tube collector featuring a helically coiled wire with a diameter of 1.5 mm placed within the inner glass tube. The wire diameter is set at 1.5 mm, taking into account the thickness of the laminar sublayer for airflow. Through this enhancement, they realized improvements in air temperature increase and efficiency of 7.3 °C and 2.1%, respectively, when compared to those of basic ETC. Al-Joboory [6] conducted a comparative analysis of thermosyphon ETC and ETC featuring 20 wickless heat pipes for use in water heating applications. They utilized methanol as the heat transfer fluid in the heat pipe, maintaining a 50% filling ratio. It was determined that the ETC with heat pipe demonstrated enhanced efficiency compared to the thermosyphon ETC, with improvements of 22.5%, 42.5%, and 32.4% at no load, intermittent load, and continuous load, respectively. Manoj Kumar and colleagues [7] examined the thermal storage properties of PCM embedded with nanoparticles. They employed paraffin as the base material and CeO2 as the nanoparticle material in three distinct mass fractions: 0.5%, 1.0%, and 2.0%. They noted considerable enhancement in the storage properties of the PCM with nanoparticles in comparison to standard paraffin, with the greatest enhancement seen in the 1.0% nanoparticle-embedded paraffin PCM. Wang et al. [8] created a network of 10 connected ETCs featuring a copper U-shaped tube installed within. All 10 ETCs utilized a simplified compound parabolic concentrator. Experimental and computational investigations have been conducted. They achieved air outlet temperatures above 200 °C with a mass flow rate between 6.8 m^3/hr. [9] introduced a SAH system comprising 30 connected identical ETCs and discovered that as the number of units rises, the maximum outlet air temperature increases while the thermal efficiency declines. The thermal efficiencies were recorded as 52%, 35%, and 21% for air outlet temperatures of 70 °C, 150 °C, and 220 °C, respectively, at a steady mass flow rate of 25 m^3/hr. Wannagosit et al. [10] conducted both an experimental and computational investigation for heating water with ETC. They utilized 8 ETC featuring a thermosiphon heat exchanger containing "R-141 b" with a 70% filling ratio. They achieved thermal efficiency and peak water temperature of 58.28% and 96.45% respectively. Mohamed et al. [11] conducted a comparative experimental investigation on the performance of ETC utilizing heat pipes without fins, traditional longitudinal fins, and innovative helical fins for water heating purposes. Paraffin was utilized as PCM and tap water as HTF, with mass flow rates varying from 0.165 LPM to 0.665 LPM. They discovered that employing finned heat pipes greatly improves the performance of ETC relative to that without fins. The helical finned heat pipe system improves daily thermal efficiency compared to a conventional finned system by 15% and 13.6% at water mass flow rates of 0.5 LPM and 0.665 LPM, respectively. Dinesh et al. [12] conducted experiments to examine the performance improvement of ETC by employing diffuse reflectors beneath the ETC tubes for water heating purposes. They employed two distinct reflectors, specifically Flat Diffuse Reflector and Wavy Diffuse Reflector, alongside a water tank with a capacity of 100 litres. They achieved a tank water temperature increase of 4 0C and 6 0C using Flat and wavy diffuse reflectors, respectively. Gunasekaran et al. [13] conducted experimental research on the performance improvement of ETC by utilizing twisted tape inserts for water heating purposes. They utilized 15 copper tape.

Veera Kumar et al [14] conducted an analytical study on the impact of different configurations of twisted tape inserts for air heating purposes. Out of 10 distinct configurations, it was discovered that the loose fit perforated twisted tape (LFPTT) outperformed the others, leading to its selection for further analysis to determine the twist ratio (y/D) and the tape hole diameter ratio (d/D). They achieved the highest thermal efficiency of 62.3% at 400 kg/hr utilizing LFPTT with (y/D) = 2 and (d/D) = 0.0714. Mohammed et al. [15] conducted experiments to examine the impact of incorporating PCM in ETC and supplementary PCM tanks within the water storage tanks on the efficiency of ETC for water heating purposes. They employed heat pipes containing acetone within the ETC and utilized paraffin as PCM in both the ETC and water tanks. They achieved the maximum efficiency of 89.97% and 91.16% with water mass flow rates of 1 LPH and 2 LPH, respectively, using PCM in both ETC and the water tank. Afshari et al. [16] introduced a budget-friendly solar air heater design lacking insulation featuring various turbulators. They utilized sheet metal measuring 90 cm in length and tubes with a diameter of 9.5 cm, all coated with matte black paint. They created these tubes in U shapes by utilizing elbows to shorten their total length. They conducted both computational and experimental studies using three distinct turbulator configurations. By arranging

the turbulators in two opposing rows, they achieved a peak instantaneous heater efficiency of 72.41%. Johane et al. [17] explored both computationally and experimentally the influence of collector tilt angle on the efficiency of ETC for water heating purposes. They utilized 8 water in glass ETCs with a 40-liter capacity water storage tank. Antonio et al. [19] introduced a novel solar air heating system that employs direct air heating within the linear concentrating collectors. They conducted a numerical analysis to assess the performance of this system utilizing a Brayton cycle with a compression ratio ranging from 1.5 to 4, alongside Linear Fresnel collector and parabolic trough collector. Their research showed that this system operates without needing an external power source and can deliver air temperatures of 300-400 °C for different industrial uses. Mehla et al. [20] conducted experiments to explore how used engine oil as a storage medium impacts the performance of ETC in air heating applications. Twenty ETC tubes were utilized, each featuring circular fins and filled with used engine oil. They conducted the experiments in winter for 13 hours of air heating using different mass flow rates. They discovered that the highest temperature difference of 24.8 °C occurs at a low airflow rate of 79.5 kg/hr, while the peak average efficiency of 28.8% is achieved at a high airflow rate of 159 kg/hr using a circular fin and counterflow setup. Muhammed et al. [21] examined how nanofluids within the ETC influence performance for water heating applications. They utilized water-based nanofluids, specifically AL2O3-H2O and CuO-H2O. They utilized two distinct fluid flow circuits: one with nanofluid within an ETC and the other with water circulating in a tank. They found that the CuO-H2O nanofluid shows a notable enhancement in performance. Olfian et al. [22] discussed recent advancements and various modifications employed in ETC, as well as the applications of different kinds of nanofluids in ETC. They outlined the applications of various nanoparticle types, their size ranges and concentrations, and their impacts on the thermal performance of ETC. Agrawal et al. [23] and Amit Kumar et al. [24] presented a review of recent advancements in ETC utilizing various modification and augmentations such as use of nanofluids as PCM, tilt angle, reflectors etc on the performance of ETC for water and air heating applications.

2. Experimental Setup

The schematic and the pictorial view of the experimental setup is shown figure 1. It has a frame containing a header at its top. The upper member of the frame is inclined at an angle of 220 resembling the latitude angle of Bilaspur. A standard glass evacuated tube is used whose specifications are mentioned in table 1. Open end of the ETC is inserted inside the header and other side rests on the supports provided on the frame. Here, inside the ETC the conventional U tube type arrangement is made in which a thin copper sheet of 0.3 mm thickness in the form of a co-axial cylinder touching the inner surface of the ETC is inserted. A copper U tube of inner and outer diameters of 11 mm and 13 mm respectively is placed inside the ETC firmly touching the inner surface of the copper sheet. The two ends of the U tube coming out in the header from the ETC are connected to inlet side and outlet side respectively through 0.5 Inch diameter galvanized iron pipe fittings. The inlet pipe to the ETC is connected to a blower to supply air to ETC. here, blower supplies ambient air at different mass flow rates to ETC which gets heated up by absorbing the solar radiation through the ETC and the hot air is taken out through the outlet manifold. K-type thermocouples are placed at the inlet; outlet and different locations of ETC. Thermocouples are connected to 12 channel temperature indicator to measure temperature of various locations of the set up.

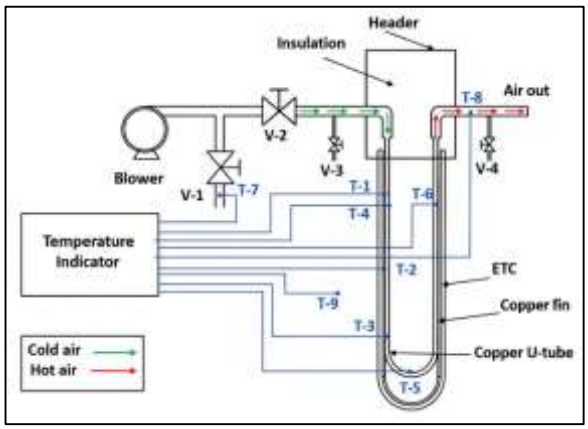

(a)



(b)

Figure 1. *Experimental setup (a) Schematic (b) Pictorial view.*

The pressure drop across the ETC is measured using differential pressure manometer. Intensity of the solar radiation was measured with the help of solar power meter. Anemometer is used to find the velocity at the exit of the ETC from which mass flow rate through the ETC was calculated. Experiments were performed on different days when sky was clear from November 2024 to May 2025. Temperature indicator is connected to K-type thermocouples associates with nine different locations of set up details of which are as follows. T1, T2, T3 - three different axial points on copper sheet, T4 - inlet side of the copper tube, T5 - middle of copper tube, T6 - outlet side of the copper tube, T7 - air temperature at ETC inlet, T8 - air temperature at ETC outlet, T9 - ambient temperature. Table 1 presents specifications of a standard evacuated tube collector (ETC) used for present study.

Table 1. *Specifications of evacuated tube collector (ETC).*

Properties	Descriptions
Material	Borosilicate Glass
Length (mm)	1800
Outer diameter (mm)	58
Inner diameter (mm)	47
Coating Material	ALN/AIN-SS/CU
Absorptance	> 92%
Emittance	< 8%
Transmittance	>89%
Vacuum (Pa)	5 x 10 $^{-3}$

2.1 Mathematical Equations

Performance parameters of solar ETC air heater are expressed as temperature rise, collector efficiency, exergy efficiency and pressure drop across the ETC. It was assumed that the heat absorbed by the absorber tube is completely transferred to the air flowing through the ETC. specific heat of air is taken to be constant throughout the temperature range.

The temperature rise across the ETC have been calculated by the difference in the temperatures of air at inlet and the outlet. It can be expressed as

Temperature rise:

$$\Delta T = (T_8 - T_7) \quad (1)$$

The collector efficiency or thermal efficiency is expressed as the ratio of heat gained by the air to the solar radiation energy incident on the ETC surface.

Collector efficiency:

$$\eta_{th} = \frac{\dot{m} C_p \Delta T}{A I} \quad (2)$$

AS per MNRE guidelines, Collector area of a single tube can be obtained as Area of collector tube:

A = π x outer radius of ETC x length of the ETC (3)

Mass flow rates through ETC is obtained by measuring air velocity at the exit of the ETC and using following equation

$$\dot{m} = \rho_a V_e A_e \quad (4)$$

Blower power consumption for the specified mass flow rates have been calculated as follows.

Blower Power:

$$P = \frac{\dot{m} \Delta p}{\rho_a} \quad (5)$$

2.2 Measuring instruments

Various instruments and devices used for present study are shown in figure 2. Figure 2 (a) and (b) shows the front and back side of a 12-channel temperature indicator to measure temperatures at various locations of the set up. Figure 3 (c) represents an anemometer which is used to measure velocity and hence mass flow rate through exit of the ETC. figure 3 (d) represents the solar power meter used to measure the intensity of the solar radiation during the experiment. Tapping for pressure drop measurement has also been provided at the inlet and outlet of the ETC to which a differential pressure manometer is attached. This is used to measure the pressure drop across the ETC when the flow takes place.

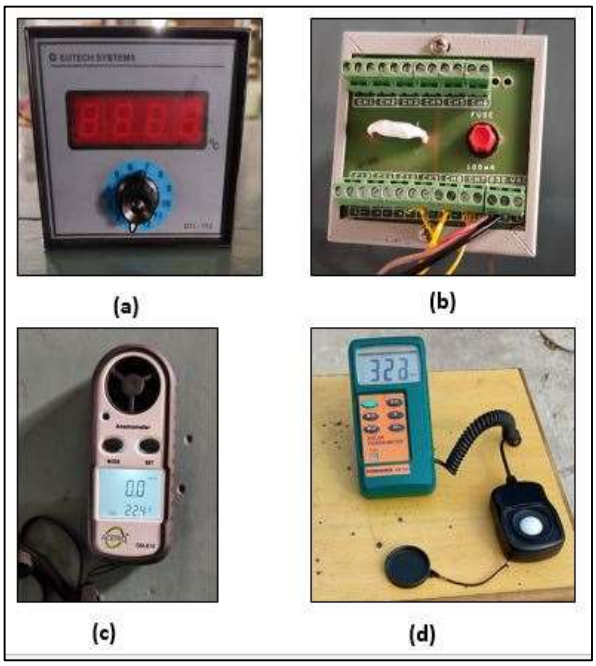

Figure 2. *Equipments used for the experiments. (a) Temperature indicator (front side), (b) Temperature indicator (back side), (c) Anemometer, (d) Solar power meter.*

3. Results and Discussion:

In the present study experiments have been performed from November 2024 to May 2025 in the local climate conditions of Bilaspur, Chhattisgarh, India from 09:00 hours to 04:00 hours. Experiments have been performed at four different air mass flow rates from 1 kg/hr to 4 kg/hr. Temperatures at three different locations on the copper fin have also been measured. It was observed from the experimental data that the temperature variation at these three locations of the copper fin is very less. Pressure drop across the ETC, and hence blower power consumption at these mass flow rates have also been calculated. The variation of average solar intensity with specific hours in a day for the month of November, February, April and May has been presented in figure 3.

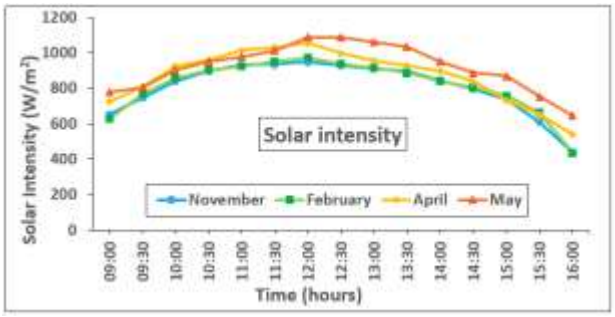

Figure 3. *Variation of solar intensity with time*

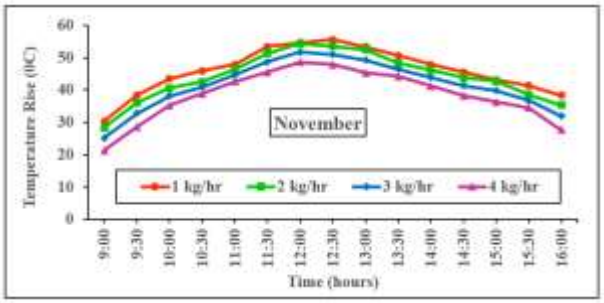

(a)

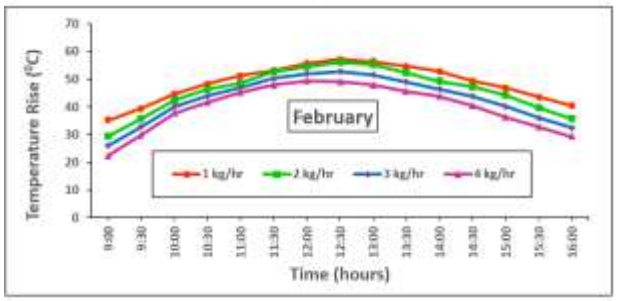

(b)

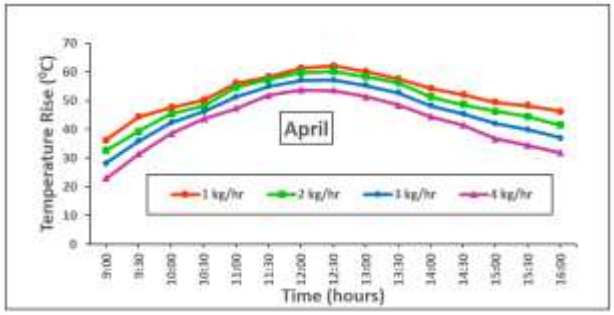

(c)

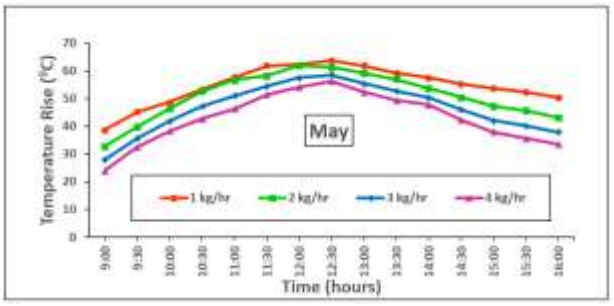

(d)

Figure 4. *Variation of temperature rise with time for different months: (a) November, (b) February, (c) April, and (d) May.*

Figure 4 and represent the variation of temperature rise across the ETC for different months at four distinct mass flow rates.

For the all the cases the temperature rise gradually increases with time, reaching its maximum value around the noon hours and slowly declines in the afternoon hours. For all these months solar intensity increases steadily, reaching its peak at noon and slowly declines during the afternoon hours. The monthly average value of maximum solar intensity was found to be 950 W/m^2, 973 W/m^2, 1055 W/m^2 and 1088 W/m^2 for the month of November, February, April and May, respectively.

It can be observed from figure 4 that as the mass flow rates through the ETC decreases the temperature rise increases. This is due to the fact that with increase in mass flow rates through the ETC minimises the time interaction of the air molecules with the ETC. however the rate of increase of the temperature rise reduces with decrease in mass flow rate. The maximum temperature rise recorded corresponding 55.5 ^{0}C, 57.2 ^{0}C, 61.1 ^{0}C and 63.7 ^{0}C for the month of November, February, It can be noticed that for the month of May temperature rise is greatest among above months. This is due to the fact that the solar intensity is highest for the month of May among above four months.Figure 5 shows the variation of the average copper fin temperature for four different months at four distinct mass flow rates. Fin temperature resembles the ETC absorber tube temperature. The higher the value of copper fin temperature higher will be the heat loss form the ETC to the ambient. Figure 6 shows that the fin temperature is a strong function of solar intensity and follows a similar trend as that of solar intensity with time. Furthermore, decrease in the mass flow rate increases the copper fin temperature very rapidly. The maximum average fin temperatures were found to be 148.0 ^{0}C, 163.7 ^{0}C, 172.3 ^{0}C and 178.0 ^{0}C for the month of November, February, April and May respectively corresponding to the mass flow rates of 1 kg/hr.

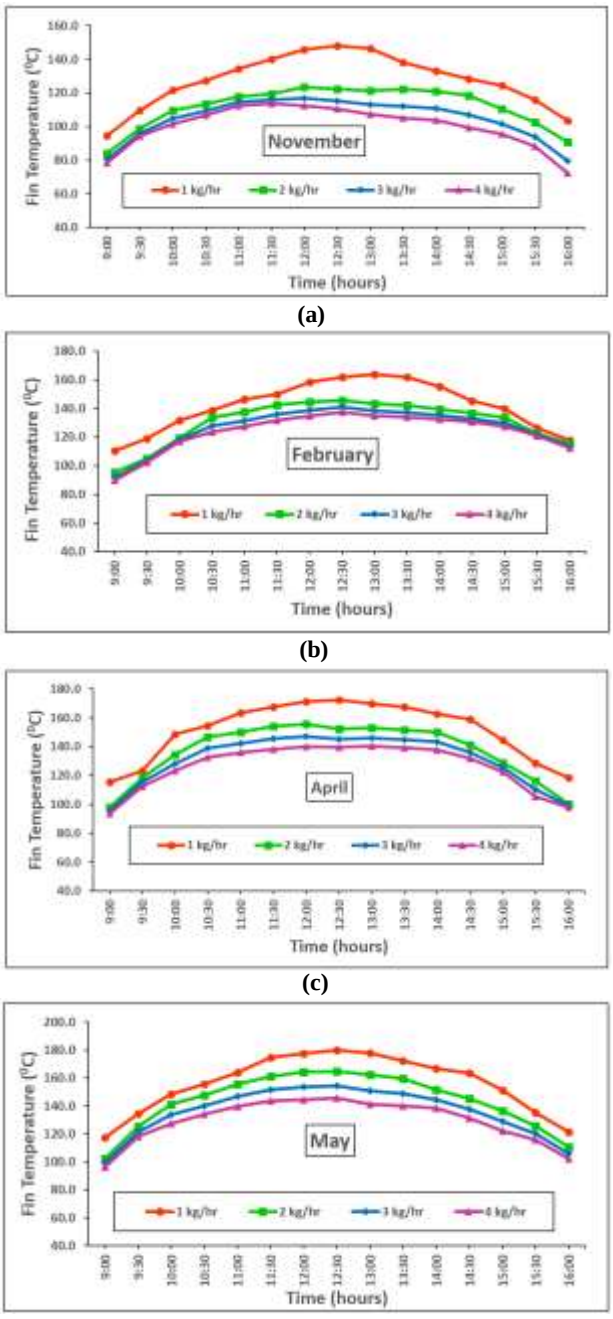

Figure 5. *Variation of copper fin temperature with time: (a) November, (b) February, (c) April, and (d) May.*

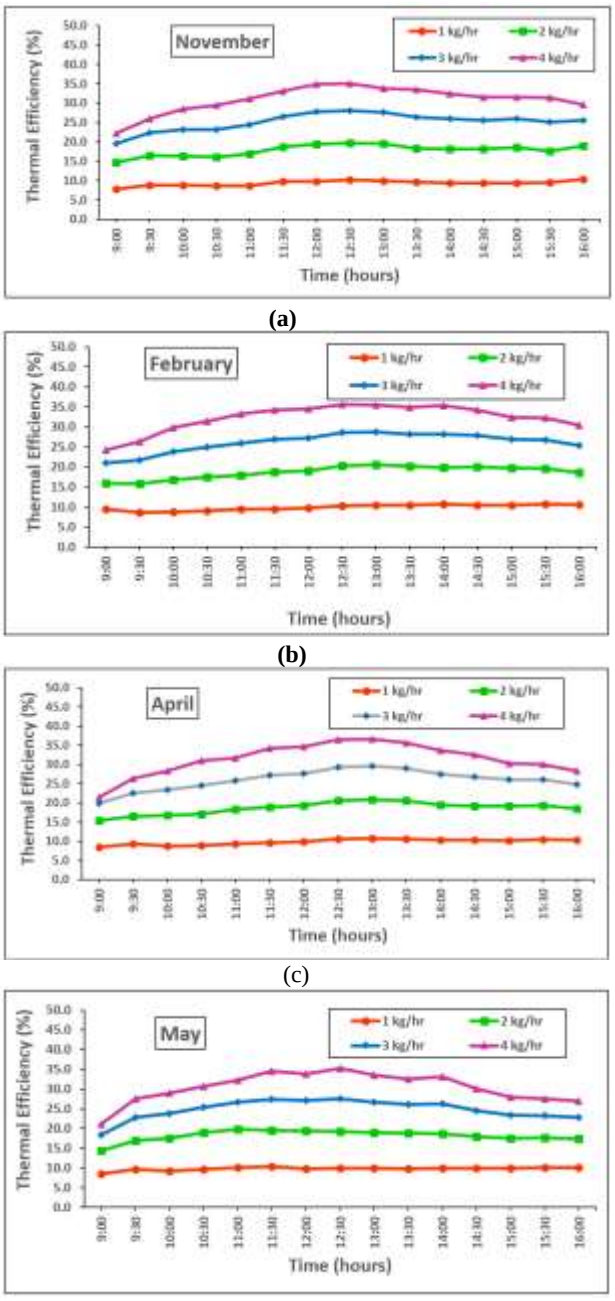

Figure 6. *Variation of thermal efficiency with time: (a) November, (b) February, (c) April, and (d) May.*

Figure 6 represents the variation of thermal efficiency with time. Thermal efficiency assesses the ratio of useful heat gain by the ETC to the total incident solar radiation on the ETC. As depicted by the graphs that the thermal efficiency increases slowly with time reaching its peak around noon hours and declining slowly in the afternoon. However, at low mass flow rates, the maximum efficiency occurs in the afternoon. It can further be observed from Figure 6 that as the mass flow rate through the ETC increases, thermal efficiency increases due to an increase in useful heat gain from the ETC.

The average maximum value of thermal efficiencies was evaluated to be 35.0%, 35.5%, 36.6% and 35.2% for the months of November, February, April and May, respectively, corresponding to the mass flow rates of 4 kg/hr.Table 2 shows the variation of pressure drop and blower power consumed across the ETC. it clearly shows that the pressure drops and blower power both increases rapidly with increase in mass flow rates. This is due to the fact that the increase in mass flow rate increases the Reynolds number and hence turbulence level of the flow. The pressure drop and blower power were found to be 0.06 KPa and 0.01 W respectively corresponding to the mass flow rate

Table 2. *Variation of pressure drop and blower power with mass flow rate.*

Mass flow rates (kg/hr)	Pressure drop (KPa)	Blower power (W)
1.0	0.06	0.01
2.0	0.14	0.07
3.0	0.22	0.16
4.0	0.3	0.31

of 1 kg/hr however the pressure drop and blower power rapidly increases to 0.3 KPa and 0.31 W respectively corresponding to the air mass flow rate of 4 kg/hr.

3.1 Uncertainty analysis:

Due to uncertainty in the measurement of various parameters during the experiment uncertainty analysis is done. These errors are due to various unavoidable instrumental, operational or operational factors associated with the measurement of various parameters during the experiment. Uncertainty analysis predicts about the uncertainty associated with the dependent variable by taking into account the uncertainty associated with various independent variables involved. In present study dependent variables are temperature rise (ΔT) and thermal efficiency (η_{th}) however the independent variables are air velocity at the exit of the ETC (V_e), temperatures at the inlet & outlet to the ETC (T_7) & (T_8) respectively and solar intensity (I). Uncertainty in thermal efficiency is found using equation 6.

Uncertainty in thermal efficiency:

$$\eta_{th} = \sqrt{\left[\left(\frac{\partial \eta}{\partial V} X_V\right)^2 + \left(\frac{\partial \eta}{\partial T_7} X_{T_7}\right)^2 + \left(\frac{\partial \eta}{\partial T_8} X_{T_8}\right)^2 + \left(\frac{\partial \eta}{\partial I} X_I\right)^2\right]} \qquad (6)$$

Where X_V, X_{T7}, X_{T8} and X_I are the uncertainties in velocity, inlet and outlet temperatures of ETC and in solar intensity respectively. Values of the uncertainties of air velocity, temperatures and solar intensity were found to be 3%, 1% and 5% respectively. Using equation (8) the uncertainties in the temperature rise and thermal efficiency were calculated to be 2.3% and 8.7% respectively.

4. Conclusion

In present study the performance of ETC using U shaped copper tube have been examined in local condition of Bilaspur, Chhattisgarh, India in four different months from November 2024 to May 2025 at four distinct mass flow rates. Based on the results obtained in the study following conclusions can be drawn:

1. In Bilaspur local condition the peak solar intensity in month of November, February, April and May were 950 W/m2, 973 W/m2, 1055 W/m2 and 1088 W/m2 respectively which can be considered as fairly good intensity for the application of various solar energy equipment.
2. As the time during the day progresses the temperature rise increases, reaching its peak around the noon time and slowly declines in the afternoon hours. With increase in mas flow rates through the ETC, temperature rise decreases. Further, the highest value of temperature rise obtained May month as compared to other months because of highest value of solar intensity in the month of May.
3. Decreasing the air mass flow rate to 1 kg/hr shows insignificant increase in temperature rise compared to 2 kg/hr however the copper fin temperature increases very rapidly.
4. As the mass flow rate increases thermal efficiency of the ETC increases since with the increase in mass flow rates, greater amount of thermal energy from the ETC are extracted by the air.
5. The pressure drop and blower power both increases rapidly with increase in mass flow rates.

4.1 Future scope of the work:

In present study, experiments have been done in four different months of November, February, April and May at four distinct mass flow rates. In order to analyse the performance of ETC experiments may be performed in a greater number of months throughout the year. Moreover, a computational or analytical model may be developed to support the obtained experimental results.

References

[1]. Sukhatme, S. P., & Nayak, J. K. (2015). Solar energy (3rd ed.). McGraw Hill Education (India).
[2]. Kalogirou, S. A. (2014). Solar energy engineering (2nd ed.). Academic Press.
[3]. Bakry, A. I., EL-Samadony, Y. A. F., El-Agouz, S. A., Alshrombably, A. M., Abdelfatah, K. S., & Said, M. A. (2018). Performance of the one-ended evacuated tubes as medium temperature solar air heaters at low flow rates. Sustainable Energy Technologies and Assessments, 30, 174-182.
[4]. Wang, Z., Diao, Y., Zhao, Y., Chen, C., Liang, L., & Wang, T. (2020). Thermal performance of integrated collector storage solar air heater with evacuated tube and lap joint-type flat micro-heat pipe arrays. Applied Energy, 261, 114466.
[5]. Singh, I., & Vardhan, S. (2021). Experimental investigation of an evacuated tube collector solar air

heater with helical inserts. Renewable Energy, 163, 1963-1972.

[6]. Al-Joboory, H. N. S. (2019). Comparative experimental investigation of two evacuated tube solar water heaters of different configurations for domestic application of Baghdad, Iraq. Energy & Buildings, 203, 109437.

[7]. Kumar, P. M., & Mylsamy, K. (2020). A comprehensive study on thermal storage characteristics of nano-CeO_2 embedded phase change material and its influence on the performance of evacuated tube solar water heater. Renewable Energy, 162, 662-676.

[8]. Wang, P.-Y., Guan, H.-Y., Liu, Z.-H., Wang, G.-S., Zhao, F., & Xiao, H.-S. (2014). High temperature collecting performance of a new all-glass evacuated tubular solar air heater with U-shaped tube heat exchanger. Energy Conversion and Management, 77, 315-323.

[9]. Wang, P.-Y., Li, S.-F., & Liu, Z.-H. (2015). Collecting performance of an evacuated tubular solar high-temperature air heater with concentric tube heat exchanger. Energy Conversion and Management, 106, 1166-1173.

[10]. Wannagosit, C., Sakulchangsatjatai, P., Kammuang-lue, N., & Terdtoon, P. (2018). Validated mathematical models of a solar water heater system with thermosyphon evacuated tube collectors. Case Studies in Thermal Engineering, 12, 528-536.

[11]. Essa, M. A., Rofaiel, I. Y., & Ahmed, M. A. (2020). Experimental and theoretical analysis for the performance of evacuated tube collector integrated with helical finned heat pipes using PCM energy storage. Energy, 206, 118166.

[12]. D. S. N., R. S., Kumar, P. M., Subbiah, R., Karthick, A., & S. P. T. (2021). Study on an ETC solar water heater using flat and wavy diffuse reflectors. Materials Today: Proceedings, 47, 5228-5232.

[13]. Gunasekaran, N., Kumar, P. M., Raja, S., Sharavanan, S., Avinas, K., Aakash Kannan, P., & Gokul, S. (2021). Investigation on ETC solar water heater using twisted tape inserts. Materials Today: Proceedings, 47, 5011-5016.

[14]. Veera Kumar, A., Arjunan, T. V., Seenivasan, D., Venkatramanan, R., Vijayan, S., & Matheswaran, M. M. (2021). Influence of twisted tape inserts on energy and exergy performance of an evacuated tube-based solar air collector. Solar Energy, 225, 892-904.

[15]. Alshukri, M. J., Eidan, A. A., & Najim, S. I. (2021). Thermal performance of heat pipe evacuated tube solar collector integrated with different types of phase change materials at various locations. Renewable Energy, 171, 635-646.

[16]. Afshari, F., Seozen, A., Khanlari, A., Tuncer, A. D., & Sirin, C. (2020). Effect of turbulator modifications on the thermal performance of cost-effective alternative solar air heater. Renewable Energy, 158, 297-310.

[17]. Bracamonte, J., Parada, J., Dimas, J., & Baritto, M. (2015). Effect of the collector tilt angle on thermal efficiency and stratification of passive water in glass evacuated tube solar water heater. Applied Energy, 155, 648-659.

[18]. Elarem, R., Alqahtani, T., Mellouli, S., Aich, W., Khedher, N. B., Kolsi, L., & Jemni, A. (2021). Numerical study of an evacuated tube solar collector incorporating a Nano-PCM as a latent heat storage system. Case Studies in Thermal Engineering, 24, 100859.

[19]. Famiglietti, A., Lecuona-Neumann, A., Nogueira, J., & Rahjoo, M. (2020). Direct solar production of medium temperature hot air for industrial applications in linear concentrating solar collectors using an open Brayton cycle viability analysis. Applied Thermal Engineering, 169, 114914.

[20]. Mehla, N., & Kumar, A. (2021). Experimental evaluation of used engine oil based thermal energy storage coupled with novel evacuated tube solar air collector (NETAC). Journal of Energy Storage, 39, 102656.

[21]. Mercan, M., & Yurddaş, A. (2019). Numerical analysis of evacuated tube solar collectors using nanofluids. Solar Energy, 191, 167–179.

[22]. Olfian, H., Mousavi Ajarostaghi, S. S., & Ebrahimnataj, M. (2020). Development on evacuated tube solar collectors: A review of the last decade results of using nanofluids. Solar Energy, 211, 265-282.

[23]. Aggarwal, S., Kumar, S., Kumar, R., & Thakur, R. (2021). Thermal augmentation in evacuated tube solar collectors using reflectors, nanofluids, phase change materials and tilt angle: A review. Materials Today: Proceedings, 45, 4931-4935.

[24]. Kumar, A., Tiwari, A. K., & Said, Z. (2021). A comprehensive review analysis on advances of evacuated tube solar collector using nanofluids and PCM. Sustainable Energy Technologies and Assessments, 47, 101417.

[25]. Plante, R. H. (2014). Solar energy, photovoltaics, and domestic hot water: A technical and economic guide for project planners, builders, and property owners. Academic Press.

[26]. Kalogirou, S. A. (2004). Solar thermal collectors and applications. Progress in Energy and Combustion Science, 30(3), 231-295.

[27]. Kim, Y., & Seo, T. (2007). Thermal performances comparisons of the glass evacuated tube solar collectors with shapes of absorber tube. Renewable Energy, 32(5), 772-795.

[28]. Speyer, E. (1965). Solar energy collection with evacuated tubes. Journal of Engineering for Power, 87(3), 270–276.

[29]. Gong, J. H., Jiang, Z., Luo, X. F., et al. (2020). Straight-through all-glass evacuated tube solar collector for low and medium temperature applications. Solar Energy, 201, 935-943.

[30]. Siuta-Olcha, A., Cholewa, T., & Dopieralska-Howoruszko, K. (2021). Experimental studies of thermal performance of an evacuated tube heat pipe solar collector in Polish climatic conditions. Environmental Science and Pollution Research, 28, 14319-14328.